

MODEL OF PULVERIZED COAL COMBUSTION IN A FURNACE

ROBERT STRAKA AND JINDŘICH MAKVIČKA

We describe behavior of the air-coal mixture using the Navier–Stokes equations for gas and particle phases, accompanied by a turbulence model. The undergoing chemical reactions are described by the Arrhenian kinetics (reaction rate proportional to $\exp(-\frac{E}{RT})$, where T is temperature). We also consider the heat transfer via conduction and radiation. Moreover we use improved turbulence-chemistry interactions for reaction terms. The system of PDEs is discretized using the finite volume method (FVM) and an advection upstream splitting method as the Riemann solver. The resulting ODEs are solved using the 4th-order Runge–Kutta method. Sample simulation results for typical power production levels are presented.

Keywords: turbulence, heat transfer, combustion, NOx

AMS Subject Classification: 35L65, 76M12, 80A20

1. INTRODUCTION

The main motivation of the combustion model research is its future inclusion in the current model of the steam generator (see [9] and also [1]), to use this model for development of control systems for the industrial installation. Another purpose for the combustion model is the optimization of the production of the nitrogen oxides, which strongly depends on the temperature distribution, and thus can be controlled by intelligent distribution of fuel and oxygen into the burners. Because the experiments on a real device are prohibitively cumbersome and expensive, in extreme cases even hazardous, the only way to test the behavior of the furnace is mathematical modeling.

An industrial pulverized coal furnace is basically a vertical channel with square cross-section. The dimensions are determined by the power generation requirements from the order of meters to tens of meters. In the case we model, the furnace has 30 meters in height and 7 meters in width, 49 m² cross-section. Power production of such a furnace is about 90 MW, and the furnace coupled with a steam generator is capable of producing about 100 tons of pressurized superheated steam per hour.

In the bottom of the channel walls, there are several burners – jets where the mixture of the air and coal powder is injected. The mixture then flows up and

burns, while it transfers some of the combustion heat to the walls containing the water pipes.

At the top, the heated flue gas continues to flow to the superheater channel where further heat exchange occurs, and this has already been covered by [9]. Our main concern is now modeling of the processes in the area, where the coal gets burnt and nitric oxides are produced.

2. MATHEMATICAL MODEL

The mathematical model of combustion is based on the Navier-Stokes equations for a mixture of multiple components where the coal particle are treated as one of the phases. Thus, the model belongs to the class of multi-phase problems (see also [10]). Unlike e.g. in [3], where the gas particles are treated separately and use separate equations of momentum, we chose to use this approach, as it simplifies the model especially when dealing with turbulence, and also removes several empirical relations and constants.

Currently, the following components of the mixture are considered:

- chemical compounds engaged in major thermal and fuel NOx reactions: nitrogen (N_2), oxygen (O_2), nitric oxide (NO), hydrogen cyanide (HCN), ammonia (NH_3), and water (H_2O)
- char and volatile part of the coal particles.

The gas phase is described by the following equations. As stated above, the mass balance is described by equations of mass balance of each subcomponent (the Einstein summation is used)

$$\frac{\partial}{\partial t}(\rho Y_i) + \frac{\partial}{\partial x_j}(\rho Y_i u_j) = \nabla \vec{J}_i + R_i, \quad (1)$$

where ρ is the flue gas mass density, Y_i concentration of the component, and u_j are the gas velocity components. The right-hand side terms describe the laminar and turbulent diffusion of the components and either production or consumption due to chemical reactions within the R_i term.

The above equations of component mass balance are accompanied by the equation of total mass balance

$$\frac{\partial \rho}{\partial t} + \frac{\partial(\rho u_j)}{\partial x_j} = 0. \quad (2)$$

Equations of momentum conservation are as follows

$$\frac{\partial}{\partial t}(\rho u_i) + \frac{\partial}{\partial x_j}(\rho u_i u_j) = -\frac{\partial p}{\partial x_i} + \frac{\partial}{\partial x_j} \left[\mu_{\text{eff}} \left(\frac{\partial u_i}{\partial x_j} + \frac{\partial u_j}{\partial x_i} - \frac{2}{3} \delta_{ij} \frac{\partial u_l}{\partial x_l} \right) \right] + g_i, \quad (3)$$

where $\vec{g} = [g_1, g_2, g_3]$ is the external force acting on the fluid, in our case the gravity. The effective friction coefficient μ_{eff} is calculated from the turbulence model as

$$\mu_{\text{eff}} = \mu + \mu_t = \mu + \rho C_\mu \frac{k^2}{\epsilon},$$

where μ is the laminar viscosity, k the turbulent kinetic energy, and ϵ the turbulent energy dissipation rate. Constant C_μ , like additional constants mentioned later in the description of the turbulence model, has to be chosen empirically for the particular problem, in our case we use $C_\mu = 0.09$, which appears to give satisfactory results. All empirical constants in the turbulence model stated here are taken from [16].

The last equation describes the conservation of energy

$$\frac{\partial}{\partial t}(\rho h) + \frac{\partial}{\partial x_j}(\rho u_j h) = -n_p \frac{dm_p}{dt} h_{\text{comb}} + q_r + q_c + q_s, \tag{4}$$

where the right-hand side terms are the heat of combustion, heat transfer by radiation, heat transfer by conduction, and heat source or sink. The heat transfer terms are computed as follows

$$-q_c = \nabla \cdot (\lambda \nabla T),$$

for the transfer by conduction, which is described by the Fourier law of heat conduction, and

$$-q_r = \nabla \cdot (cT^3 \nabla T),$$

for the transfer by radiation. The radiation heat transfer is fully described by an integral-differential equation of radiation, which is very computationally expensive to solve. However, as the flue gas can be considered an optically thick matter, the above approximation of the radiation flux called Rosseland radiation model can be applied [16].

The heat sink term is nonzero only in the edge computation cells and describes the energy exchange with the walls of the furnace via conduction and radiation

$$q_s = A(T_{\text{gas}} - T_{\text{wall}}) + B(T_{\text{gas}}^4 - T_{\text{wall}}^4),$$

where A and B are constants dependent on the properties of the interface between the modeled region and its surroundings.

The particle mass change rate is currently described by one-step Arrhenian kinetics, which is used separately for the char and volatile coal components – combustion of the volatiles is more rapid than combustion of the char

$$\frac{dm_p}{dt} = -A_v m_p^\alpha [\text{O}_2]^\beta \exp\left(-\frac{E_v}{RT_p}\right),$$

where m_p is the particle combustible mass, A_v , E_v , α , β are empirical constants, $[\text{O}_2]$ oxygen concentration and T_p is the particle temperature.

These equations are accompanied by the equation of state, as usually

$$p = (\kappa - 1)\rho_{\text{gas}} \left(e_{\text{gas}} - \frac{1}{2}v_{\text{gas}}^2 \right).$$

Here, κ is the Poisson constant and e_{gas} is the gas energy per unit mass.

For the turbulence modeling, we use the standard k - ϵ model, which describes the evolution of turbulence using two equations – first one for turbulent kinetic energy

$$\frac{\partial}{\partial t}(\rho k) + \frac{\partial}{\partial x_j}(\rho k u_j) = \frac{\partial}{\partial x_j} \left[\left(\mu + \frac{\mu_t}{\sigma_k} \right) \frac{\partial k}{\partial x_j} \right] + G_k - \rho \epsilon, \tag{5}$$

and the second one for turbulent kinetic energy dissipation rate

$$\frac{\partial}{\partial t}(\rho\varepsilon) + \frac{\partial}{\partial x_j}(\rho\varepsilon u_j) = \frac{\partial}{\partial x_j} \left[\left(\mu + \frac{\mu_t}{\sigma_\varepsilon} \right) \frac{\partial \varepsilon}{\partial x_j} \right] + C_{1\varepsilon} \frac{\varepsilon}{k} G_k - C_{2\varepsilon} \rho \frac{\varepsilon^2}{k}. \quad (6)$$

Constants in this model have again to be determined empirically, in our case we use the following values: $C_{1\varepsilon} = 1.44$, $C_{2\varepsilon} = 1.92$, $\sigma_k = 1.0$, $\sigma_\varepsilon = 1.3$.

Left hand sides of the equations describe passive advection of the respective quantities by the advection velocity \vec{u} . Right hand sides describe their spatial diffusion, their production and dissipation.

The term G_k , which describes the production of turbulence, can be derived from the Reynolds averaging process and written in the terms of the fluctuating part of the velocity as

$$G_k = \tau_{jl} \frac{\partial u_j}{\partial x_l} = -\overline{\rho u'_j u'_l} \frac{\partial u_j}{\partial x_l},$$

where τ_{jl} is the Reynolds stress tensor. However during practical computation, fluctuations u'_j and u'_l are unknown. Using the Boussinesq hypothesis, that the Reynolds stress is proportional to the mean strain rate

$$S_{ij} = \frac{1}{2} \left(\frac{\partial u_i}{\partial x_j} + \frac{\partial u_j}{\partial x_i} \right),$$

one can write turbulent production in a closed form

$$G_k = \mu_t S^2, \quad S = (2S_{jl}S_{jl})^{1/2}.$$

Diffusion of the species consists of two processes – laminar and turbulent, and the diffusion term in Eq. (1) can be written in the form

$$\vec{J}_i = - \left(\rho D_{i,m} + \frac{\mu_t}{Sc_t} \right) \nabla Y_i.$$

First term corresponds to linear laminar diffusion, the second one to turbulent diffusion. Given the fact that the turbulent diffusion generally predominates the laminar, and the term $D_{i,m}$ is difficult to determine, the laminar diffusion can be usually ignored. The Sc_t coefficient is the turbulent Schmidt number and we put $Sc_t = 0.7$.

To be able to model the particle phase, especially surface area of the particles, we still have to track the numerical density of the particles using the equation similar to the mass balance equation

$$\frac{\partial n_p}{\partial t} + \frac{\partial(n_p u_p)}{\partial x_1} + \frac{\partial(n_p v_p)}{\partial x_2} + \frac{\partial(n_p w_p)}{\partial x_3} = 0. \quad (7)$$

3. SIMPLIFIED MODEL OF NOX CHEMISTRY

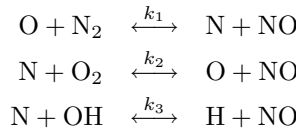
This model has been developed to approximately describe the amounts of NOx emissions leaving a coal combustion furnace. The real mechanism of coal flue gas

production seems to be very complicated, so that just the most important phenomena and reaction paths were considered to provide maximum possibility of using this model in real-time control and operation systems.

In most cases, NOx is interpreted as a group of NO and nitrogen dioxide (NO₂), which strongly pollute our living environment. There are two major processes attributing to the total NOx emitted. The former is known as *Thermal NOx* or *Zeldovich* and simply consists of oxidation of atmospheric nitrogen at high temperature conditions. The latter is called *Fuel NOx* and describes NOx creation from nitrogen, which is chemically bounded in coal fuel. Fuel NOx is usually the major source of NOx emissions. These are the only mechanisms involved, although a few more could be considered (such as *Prompt NOx (Fenimore)* or *Nitrous oxide (N₂O) intermediate* mechanisms).

3.1. Thermal NO

Thermal NO generation mechanism attributes only at high temperature conditions (~ 1800 K) and is represented by a set of three equations, introduced by Zeldovich [13] and extended by Bowman [2]



All these reactions are considered to be reversible. Rate constants were taken from [15] (see Table 1).

Table 1. Rate constants for thermal NO chemical reactions,
 $k = A \cdot T^b \cdot \exp(-E_a/T)$.

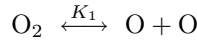
Rate const.	A	b	E _a
k ₁ ⁺	1.8 · 10 ⁸	0	38370
k ₂ ⁺	1.8 · 10 ⁴	1	4680
k ₃ ⁺	7.1 · 10 ⁷	0	450
k ₁ ⁻	3.8 · 10 ⁷	0	425
k ₂ ⁻	3.8 · 10 ³	1	20820
k ₃ ⁻	1.7 · 10 ⁸	0	24560

In order to compute the NO concentration, concentrations of nitrogen radical [N], oxygen radical [O] and hydroxyl radical [OH] must be known. It is useful to assume [N] to be in a quasi-steady state according to its nearly immediate conservation after creation. In fact, this N-radical formation is the rate limiting factor for thermal NO production, due to an extremely high activation energy of nitrogen molecule, which

is caused by a triple bond between two nitrogen atoms. Hence, NO formation rate can be stated as

$$\frac{d[\text{NO}]}{dt} = 2k_1^+ \cdot [\text{O}] \cdot [\text{N}_2] \cdot \frac{1 - \frac{k_1^- k_2^- [\text{NO}]^2}{k_1^+ [\text{N}_2] k_2^+ [\text{O}_2]}}{1 + \frac{k_1^- [\text{NO}]}{k_2^+ [\text{O}_2] + k_3^+ [\text{OH}]}}.$$

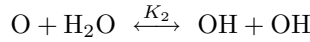
Under certain conditions, oxygen molecule splits and recombines cyclically



which can be profitably described by the following partial equilibrium approach

$$[\text{O}] = K_1 \cdot [\text{O}_2]^{1/2} \cdot T^{1/2}.$$

As for OH radical, a similar partial equilibrium approach can be made, according to next reaction



and the approach is

$$[\text{OH}] = K_2 \cdot [\text{O}]^{1/2} \cdot [\text{H}_2\text{O}]^{1/2} \cdot T^{-0.57}.$$

Equilibrium constants K_1 and K_2 are as follows

$$\begin{aligned} K_1 &= 36.64 \cdot \exp\left(\frac{-27123}{T}\right), \\ K_2 &= 2.129 \cdot 10^2 \cdot \exp\left(\frac{-4595}{T}\right). \end{aligned}$$

3.2. Fuel NO

Composition analysis show, that nitrogen-based species are more or less present in coal, usually in amounts of tenths to units of percent by weight. When the coal is heated, these species are transformed into certain intermediates and then into NO. Fuel itself is therefore a significant source of NO pollutants. When a coal particle is heated, it is presumed, that nitrogen compounds are distributed into volatiles and char. In many studies (e.g. [4]) it is unreasonably told, that half the nitrogen converts to volatiles and half into char. Since there is no reason for a presupposition like this, a parameter α is introduced to describe the distribution

$$\begin{aligned} m_{\text{vol}}^{\text{N}} &= \alpha \cdot m_{\text{tot}}^{\text{N}}, \\ m_{\text{char}}^{\text{N}} &= (1 - \alpha) \cdot m_{\text{tot}}^{\text{N}}, \end{aligned}$$

where $\alpha \in (0, 1)$, $m_{\text{tot}}^{\text{N}}$ is the total mass of nitrogen, $m_{\text{vol}}^{\text{N}}$ is the mass of nitrogen in volatiles and $m_{\text{char}}^{\text{N}}$ is the mass of nitrogen in char.

As already mentioned, nitrogen transforms to pollutants via intermediates, which usually are ammonia NH_3 and hydrocyanide HCN . For further proceeding, a selection from four possible pathways must be made (see Figure 1, ref. [11, 7]). To provide maximum complexity, another three parameters (similar to α) are introduced

- β is distribution of $m_{\text{tot}}^{\text{N}}$ between HCN and NH_3 intermediates.
- γ is distribution of $m_{\text{HCN}}^{\text{N}}$ between Pathway1 and Pathway2.
- δ is distribution of $m_{\text{NH}_3}^{\text{N}}$ between Pathway 3 and Pathway 4.
- $\beta, \gamma, \delta \in \langle 0, 1 \rangle$.

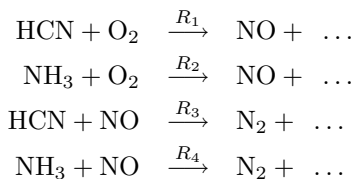
For example, mass of nitrogen in char entering Pathway 2 can be written as

$$m_{\text{P2, char}}^{\text{N}} = m_{\text{tot}}^{\text{N}} \cdot \beta \cdot (1 - \gamma) \cdot (1 - \alpha).$$

Different parametric studies should be carried out to find the best values of α, β, γ and δ suitable for specific type of coal. Five overall reactions of either NO formation or depletion were incorporated in the combustion part of the numerical code.

3.2.1. NO, HCN, NH_3 REACTIONS

According to [12], formation rates of reactions



are given as

$$\begin{aligned} R_1 &= 1.0 \cdot 10^{10} \cdot X_{\text{HCN}} \cdot X_{\text{O}_2}^a \cdot \exp\left(\frac{-33732.5}{T}\right), \\ R_2 &= 4.0 \cdot 10^6 \cdot X_{\text{NH}_3} \cdot X_{\text{O}_2}^a \cdot \exp\left(\frac{-16111.0}{T}\right), \\ R_3 &= -3.0 \cdot 10^{12} \cdot X_{\text{HCN}} \cdot X_{\text{NO}} \cdot \exp\left(\frac{-30208.2}{T}\right), \\ R_4 &= -1.8 \cdot 10^8 \cdot X_{\text{NH}_3} \cdot X_{\text{NO}} \cdot \exp\left(\frac{-13593.7}{T}\right), \end{aligned}$$

where X is the mole fraction and a is the oxygen reaction order taken from Table 2.

Table 2. Oxygen reaction order.

Oxygen mole fraction	a
$X_{\text{O}_2} \leq 4.1 \cdot 10^{-3}$	1
$4.1 \cdot 10^{-3} \leq X_{\text{O}_2} \leq 1.11 \cdot 10^{-2}$	$-3.95 - 0.9 \cdot \ln X_{\text{O}_2}$
$1.11 \cdot 10^{-2} \leq X_{\text{O}_2} \leq 0.03$	$-0.35 - 0.1 \cdot \ln X_{\text{O}_2}$
$X_{\text{O}_2} \geq 0.03$	0

Table 3. Performance for simulation on a 40×400 grid.

Nodes	Steps/s
1	2.830687
2	4.539230
4	6.394759
8	12.526646
16	22.344537
32	63.654814
64	111.208353
128	234.860252
256	304.744175

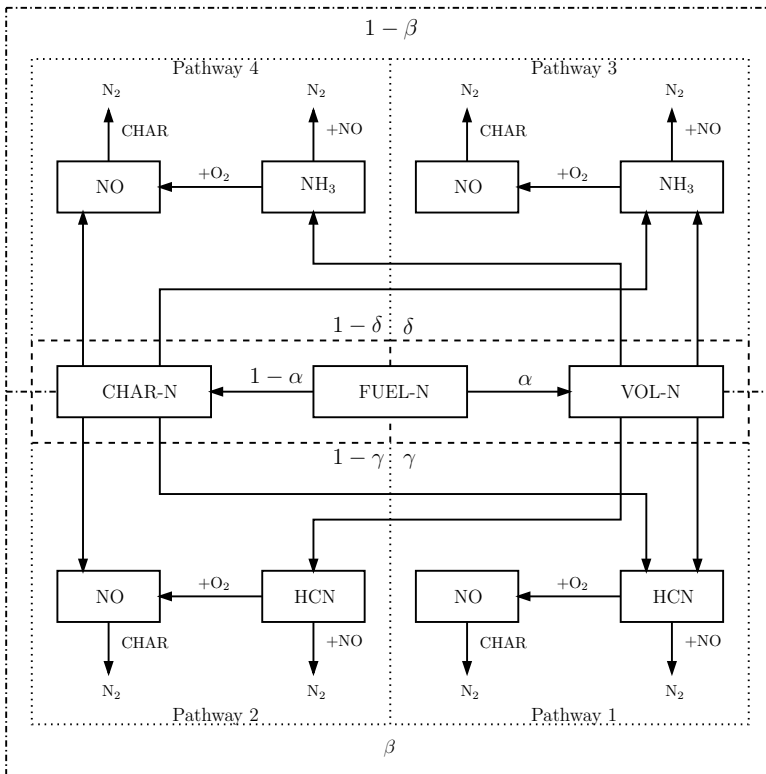
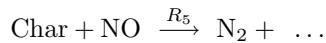


Fig. 1. Fuel NO pathways.

3.2.2. Heterogeneous NO reduction on char

Present char allows the following adsorption process to occur



Levy [5] uses pore surface area (BET) to define NO source term

$$S_{\text{ads}}^{\text{NO}} = k_5 \cdot c_s \cdot A_{\text{BET}} \cdot M_{\text{NO}} \cdot p_{\text{NO}},$$

where $k_5 = 2.27 \cdot 10^{-3} \cdot \exp\left(\frac{-17168.33}{T}\right)$ is the rate constant, $S_{\text{ads}}^{\text{NO}}$ is the NO source term, c_s is the concentration of particles, A_{BET} is the pore surface area and p_{NO} is the partial pressure of NO.

In order to evaluate overall NO source term, single source terms have to be summarized. This overall source term can be further used in transport equations. As for HCN and NH_3 source terms, it is possible to determine them from coal burnout rate. It is assumed, that nitrogen from both char and volatiles transforms to intermediate species quickly and totally.

3.3. Algebraic unified second-order moment (AUSM)

Due to complexity of chemical reactions, AUSM turbulence chemistry model is proposed by [14]. We have the following equations for time-averaged reaction rate

$$\begin{aligned} \overline{w_s} &= A\rho^2 \left[\left(\overline{Y_1 Y_2} + \overline{Y_1' Y_2'} \right) \bar{k} + \overline{Y_1 k' Y_2'} + \overline{Y_2 k' Y_1'} \right], \\ \bar{k} &= \int \exp\left(-\frac{E}{RT}\right) p(T) dT, \end{aligned}$$

when taking top-hat PDF of temperature ($p(T)$ in equation above), the time-averaged \bar{k} is

$$\bar{k} = \frac{\exp\left(-\frac{E}{R(T+g_T^{1/2})}\right) + \exp\left(-\frac{E}{R(T-g_T^{1/2})}\right)}{2},$$

where g_T is temperature correlation $g_T = \overline{T'^2}$. Correlations are determined by a generalized form of the following transport equation

$$\frac{\partial}{\partial t} (\rho \overline{\varphi \psi}) + \frac{\partial}{\partial x_j} (\rho U_j \overline{\varphi \psi}) = \frac{\partial}{\partial x_j} \left(\frac{\mu_{\text{eff}}}{\sigma_\varphi} \frac{\partial \overline{\varphi \psi}}{\partial x_j} \right) + C_{1\varepsilon} \mu_t \frac{\partial \overline{\varphi}}{\partial x_j} \frac{\partial \overline{\psi}}{\partial x_j} - C_{2\varepsilon} \frac{\varepsilon}{k} \rho \overline{\varphi' \psi'}, \quad (8)$$

where $\mu_{\text{eff}} = \mu + \mu_t$ is effective viscosity. For the sake of simplicity, (8) is reduced to the following algebraic expressions by neglecting convection and diffusion terms and assuming steady state

$$\begin{aligned} \overline{Y_1' Y_2'} &= C \frac{k^3}{\varepsilon^2} \frac{\partial \overline{Y_1}}{\partial x_j} \frac{\partial \overline{Y_2}}{\partial x_j}, & \overline{k' Y_2'} &= C \frac{k^3}{\varepsilon^2} \frac{\partial \overline{k}}{\partial x_j} \frac{\partial \overline{Y_2}}{\partial x_j}, & \overline{k' Y_1'} &= C \frac{k^3}{\varepsilon^2} \frac{\partial \overline{Y_1}}{\partial x_j} \frac{\partial \overline{k}}{\partial x_j}, \\ C &= \frac{C_{1\varepsilon}}{C_{2\varepsilon}} \rho C_\mu. \end{aligned}$$

Temperature or enthalpy fluctuation correlations g_T and g_h can be determined by

$$\begin{aligned} \frac{\partial}{\partial t} (\rho \overline{h'^2}) + \frac{\partial}{\partial x_j} (\rho U_j \overline{h'^2}) &= \frac{\partial}{\partial x_j} \left(\frac{\mu_e}{\sigma_h} \frac{\partial \overline{h'^2}}{\partial x_j} \right) + C_{1\varepsilon} \mu_t \left(\frac{\partial \overline{h}}{\partial x_j} \right)^2 - C_{2\varepsilon} \frac{\varepsilon}{k} \rho \overline{h'^2}, \\ h &= (c_p + 0.106T)T. \end{aligned}$$

4. NUMERICAL ALGORITHM

For numerical solution of the equations, finite volume method is used. For left and right hand sides in Eqs. (1), (2), (3), (4), (5), (6), (7), advection upstream splitting method (see [6]) is used to approximate fluxes in the FVM formulation, and edge dual-volume approximation is used to approximate the second order derivatives respectively. For detailed description of the solution procedure see [9].

5. PARALLELIZATION

For parallel computation of the model, MPI framework [17] has been used.

To make the above code work in parallel, each node needs to receive the data from neighboring cells of its “own” cells after each computation step. Secondly, computation of the length of the time step has to be done cooperatively using `MPI_Reduce` and `MPI_Broadcast` functions to determine the global maximum of the PDE eigenvalues.

As there are no explicit requirements on the mesh subdivision, the initialization routine has to locate all the neighbors and resolve the demands on the cells. This leads to more complicated initialization of the code, but the further communication is already simple and the code allows very general subdivisions of the grid. To test an arbitrary subdivision, even a uniform random distribution of the cells among the nodes has been tried, and the code worked, although extremely slow because of the communication overhead. For real computations, MPI functions for node distribution on Cartesian coordinates (`MPI_Cart_rank`) were used.

The demands of the cells are determined as follows: For each node, the set of cells belonging to it is expanded by a band of two cells (two neighboring cells are necessary because of the second order interpolation in the hyperbolic PDE solver). The additional cells are marked as being demanded by the node. Then, as we have for each cell a list of the nodes which demand it, we can simply build the transfer lists.

Finally, for each node, the cells are re-indexed and reallocated so the cells actually used by a node form a contiguous memory block, to maximize the CPU cache efficiency.

Although the simulation allows using an arbitrary grid, it currently uses a semi-structured grid with rectangular topology and cells narrowed at the bottom end of the furnace.

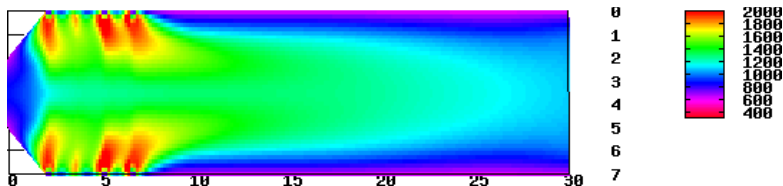


Fig. 2. Temperature profile – symmetrical channel 30×7 m, 2×4 burners, flue gas flow rate: 18 kg/s.

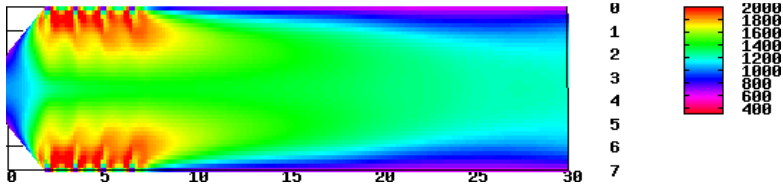


Fig. 3. Temperature profile – flue gas flow rate: 28 kg/s.

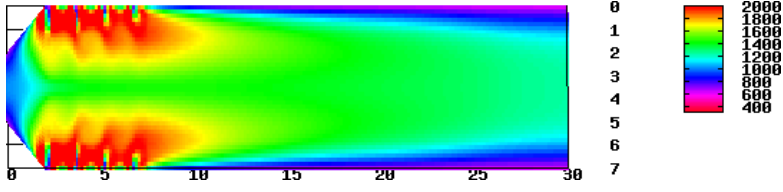


Fig. 4. Temperature profile – flue gas flow rate: 38 kg/s.

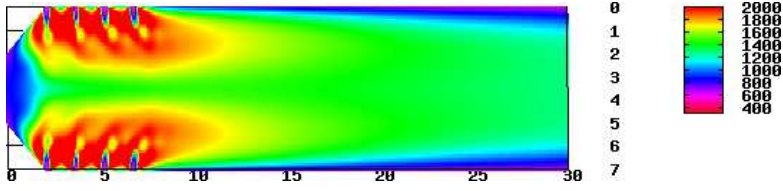


Fig. 5. Temperature profile – flue gas flow rate: 48 kg/s.

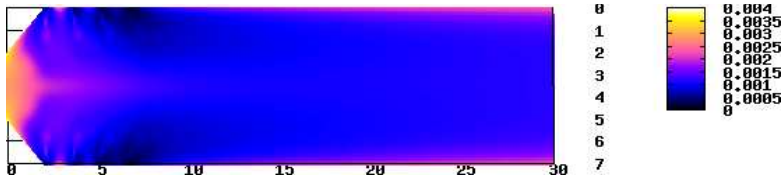


Fig. 6. NOx profile – flue gas flow rate: 48 kg/s.

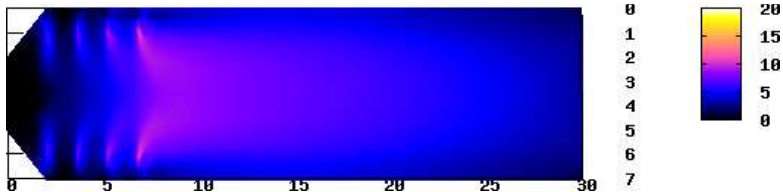


Fig. 7. Velocity profile – flue gas flow rate: 48 kg/s.

6. CONCLUSION

We have developed a mathematical model, which approximates the combustion process in an industrial furnace, while being affordable from the computational com-

plexity standpoint. Results presented in this paper are from 2D model as 3D model is being in the state of probing and development. As an outlook to the future, mainly the following improvement possibilities are being considered:

- Further refining of the coal combustion model.
- Evaluation of the NO_x generation model.
- Combustion physics enhancement.
- Heat transfer and radiation improvement.

ACKNOWLEDGEMENT

This work has been partly supported by the project MSM 6840770010 “Applied Mathematics in Physical and Technical Sciences”, and by the project LC06052 “Jindřich Nečas Center for Mathematical Modeling”, both of the Ministry of Education, Youth and Sport of the Czech Republic, and by the project “Advanced Control and Optimization for Power Generation” No. 1H-PK/22 of the Ministry of Industry and Trade of the Czech Republic.

We also would like to acknowledge the help of the HPC-Europa project, and extraordinary hospitality of the crew of CINECA supercomputer center in Bologna (Italy), where the work on the parallelization has been done. This part of the work has been performed under the Project HPC-EUROPA (RII3-CT-2003-506079), with the support of the European Community – Research Infrastructure Action under the FP6 “Structuring the European Research Area” Program.

(Received November 30, 2006.)

REFERENCES

- [1] M. Beneš and V. Havlena: Continuum Approach to the Steam Flow in a Model of Boiler. Technical Report No.1-99, Pr. 4004/99, Department of Mathematics, Faculty of Nuclear Sciences and Physical Engineering, Czech Technical University in Prague, 1999.
- [2] C. T. Bowman and D. J. Seery: Emissions from Continuous Combustion Systems. Plenum Press, New York 1972.
- [3] Y. C. Guo, C. K. Chan: A multi-fluid model for simulating turbulent gas-particle flow and pulverized coal combustion. *Fuel* 79 (2000), 1467–1476.
- [4] C. Kim and N. Lior: A numerical analysis of NO_x formation and control in radiatively/conductively-stabilized pulverized coal combustors. *Chem. Engrg. J.* 71 (1998), 221–231.
- [5] J. M. Levy, L. K. Chen, A. F. Sarofim, and J. M. Beer: NO/Char reactions at pulverized coal flame conditions. In: 18th Symposium (International) on Combustion, The Combustion Institute, Pittsburgh 1981.
- [6] M.-S. Liou and C. J. Steffen: A new flux splitting scheme. *J. Comput. Phys.* 107 (1993), 23–29.
- [7] F. C. Lockwood and C. A. Romo-Millares: The effect of particle size on NO formation in a large-scale pulverized coal-fired laboratory furnace: Measurements and modeling. *J. Inst. Energy* 93 (1992), 144–152.

- [8] J. Makovička and V. Havlena: Finite volume numerical model of coal combustion. In: Proc. Czech–Japanese Seminar in Applied Mathematics 2004 (M. Beneš, J. Mikyška, and T. Oberhuber, eds.), Faculty of Nuclear Sciences and Physical Engineering, Czech Technical University in Prague, Praha 2005, pp. 106–116.
- [9] J. Makovička, V. Havlena, and M. Beneš: Mathematical modelling of steam and flue gas flow in a heat exchanger of a steam boiler. In: ALGORITMY 2002 Proceedings of contributed papers (A. Handlovičová, Z. Krivá, K. Mikula, and D. Ševčovič, (eds.), Publ. house of STU, Bratislava 2002, pp. 171–178.
- [10] M. Beneš, T. H. Illangasekare, and J. Mikyška: On the numerical treatment of sharp texture transitions in two-phase flow. In: Czech–Japanese Seminar in Applied Mathematics 2005 (M. Beneš, M. Kimura, and T. Nakaki, eds.), COE Lecture Note Vol. 3, Hakozaki 6-10-1, Higashi-ku, Fukuoka, 812-8581, 2006, pp. 106–116. ISSN: 1881-4042. Available on-line at <http://www.math.kyushu-u.ac.jp/masato/cj/proceedings-CJ05.html>.
- [11] L. D. Smoot and P. J. Smith: Coal Combustion and Gasification. Plenum Press, New York 1985.
- [12] G. G. De Soete: Overall reaction rates of NO and N formation from fuel nitrogen. In: 15th Symposium (International) on Combustion, The Combustion Institute, Pittsburgh 1975.
- [13] Y. B. Zeldovich: The oxidation of nitrogen in combustion and explosion. *Acta Physicochimica* 21 (1946), 577–628.
- [14] L. X. Zhou, Y. Zhang, and J. Zhang: Simulation of swirling coal combustion using a full two-fluid model and an AUSM turbulence-chemistry model. *Fuel* 82 (2003), 1001–1007.
- [15] L. X. Zhou, Y. Zhang, and J. Zhang: Chemical kinetics database on the web. National Institute of Standards and Technology, 2000, <http://www.kinetics.nist.gov>.
- [16] L. X. Zhou, Y. Zhang, and J. Zhang: FLUENT User's Guide. FLUENT Inc., 2005.
- [17] L. X. Zhou, Y. Zhang, and J. Zhang: MPI: A Message-Passing Interface Standard. MPI Forum, <http://www.mpi-forum.org/docs/>.

Robert Straka and Jindřich Makovička, Department of Mathematics, Faculty of Nuclear Sciences and Physical Engineering, Czech Technical University in Prague, Trojanova 13, 120 00 Praha 2. Czech Republic.
e-mails: straka@kmlinux.fjfi.cvut.cz, makovick@kmlinux.fjfi.cvut.cz